Time-modulated oscillatory structures in phase-separating reactive mixtures

Singo Sugiura, Tohru Okuzono,* and Takao Ohta
Institute for Nonlinear Sciences and Applied Mathematics, and Department of Mathematical and Life Sciences, Graduate School of Science, Hiroshima University, Higashi-Hiroshima 739-8526, Japan
(Received 12 July 2002; revised manuscript received 21 October 2002; published 30 December 2002)

We investigate the effect of temporal modulation on the spatiotemporal patterns produced by phase separation in chemically reactive ternary mixtures. The temporal modulation is introduced by making one of the reaction rates periodic in time. Our main concern is the stability of traveling waves, which appear above a Hopf-type bifurcation at a finite wave number and are stable in the absence of external modulation. It is shown by computer simulations in two dimensions that when the external modulation is present, various types of coherent standing waves emerge near the special point in the parameter space, where the Turing-type bifurcation line and the Hopf-type bifurcation line meet each other. We carry out a theoretical analysis to understand the phase diagram of the synchronized oscillatory structures obtained numerically.

DOI: 10.1103/PhysRevE.66.066216 PACS number(s): 05.45.−a, 82.40.−g, 82.40.Ck

I. INTRODUCTION

Pattern formation far from equilibrium has been studied in various macroscopic systems such as Rayleigh-Bénard convection and the Belousov-Zhabotinsky reaction [1]. However, recently, nonequilibrium dynamics in nanoscopic or mesoscopic structures have attracted much attention because of the technical control of domains in these length scales. For instance, it has been found that reactive adsorbates on a metal surface exhibit propagating and/or standing oscillations of nanoscopic or mesoscopic domains [2,3]. Hildebrand and co-workers [4,5] have introduced a model for the traveling nanoscale stripe structures in surface chemical reactions and have successfully reproduced these dynamic behaviors by computer simulations. It is worth mentioning that a traveling mesoscopic stripe pattern has also been observed experimentally in Langmuir monolayers which undergo trans-cis transformation under ultraviolet illuminations [6]. Quite recently, this phenomenon has been studied theoretically by introducing a set of model equations, which contain a phase-separation mechanism [7].

From these examples, it is noted that phase transitions play a central role in the formation of the self-organized dynamics of microscopic domains, which is a characteristic feature in the microscopic nonequilibrium phenomena. Therefore this problem is not only relevant to industrial application but also offers a new fundamental subject of statistical physics.

In our previous paper [8] which will be referred to as I, we introduced a hypothetical reactive ternary mixture and studied a self-organized propagation of phase-separated domains. See also Ref. [9]. We consider a ternary mixture with the components A, B, and C, which undergo a chemical reaction $A \rightarrow B \rightarrow C \rightarrow A$. The reason for introducing this hypothetical cyclic linear reaction is that it is the simplest way to maintain the system far from equilibrium and hence most convenient to explore the feature of nonequilibrium systems without being involved heavily in mathematical complication. The components A and B are assumed to be phase separated at low temperature. This is modeled by the usual Cahn-Hilliard-type equation which has been studied extensively for many years [10,11].

The set of kinetic equations that consist of the Cahn-Hilliard part and the reaction terms exhibits two kinds of bifurcation depending on the parameters. One is the Turing-type bifurcation beyond which the uniform stationary state becomes unstable, and motionless periodic domain structures appear [12,13]. We do not call this bifurcation a Turing bifurcation; we call it a Turing-type bifurcation, because the original Turing bifurcation was introduced in a two-component reaction diffusion system [14], which is not the same as that studied in the present paper. The other is a Hopf-type bifurcation at a finite wave number, which is sometimes called a wave instability [4]. Throughout this paper, by a Hopf-type bifurcation, we mean a bifurcation associated with the wave instability to distinguish it from the ordinary Hopf bifurcation in a uniform system. We have found by computer simulations in two dimensions that both the stripe structure and hexagonal structure exhibit self-organized propagation at the post-threshold of the Hopf-type bifurcation. However, we have not obtained any standing oscillations of domains. This fact obtained numerically has been confirmed theoretically in the case of stripes by deriving the set of amplitude equations for traveling waves and analyzing the stability [8].

In this paper, we extend our previous study by allowing a time dependence of the reaction rates. Our main concern is how the traveling waves are destabilized by the external modulations and to see what kind of oscillations of domains appear due to the synchronization with the external modulations.

The stability of traveling waves influenced by an external temporal modulation has been studied theoretically [15] to understand the experimental observation in Rayleigh-Bénard convection of binary mixtures [16–18]. Control of Turing structures by applying an external periodic disturbance has also been investigated both theoretically and experimentally

*Present address: Yokoyama Nano-structured Liquid Crystal Project, ERATO, Japan Science and Technology Corporation, 5-9-9 Tokodai, Tsukuba 300-2635, Japan.

in chemical reactions [19,20]. It is also mentioned that various types of standing oscillations of spatially periodic structures have been observed in vibrating granular systems by changing the amplitude and frequency of vibration [21].

However, to our knowledge, there has been no intensive study of the nonequilibrium dynamical structures from the view point of entrainment by external modulations. The purpose of the present paper is to investigate the morphology and dynamics of mesoscopic domains in a phase-separated system when the reaction rates are modulated periodically in time. We will show that a variety of domain dynamics can be obtained near the multiple bifurcation point where the Hopf-type bifurcation line and the Turing-type bifurcation line meet each other.

In the following section, we shall describe our model equations for reactive ternary mixtures and summarize the previous results [8]. In Sec. III, we carry out computer simulations of the set of kinetic equations in two dimensions by introducing a time dependence of the reaction rates. A linear stability analysis based on the Floquet theorem is given in Sec. IV for the uniformly oscillating state to understand the phase diagram obtained by computer simulations. Concluding remarks and discussion are given in Sec. V.

II. CHEMICALLY REACTIVE TERNARY MIXTURES

We consider a ternary mixture composed of *A*, *B*, and *C* molecules and suppose that there is a strong repulsive short-range interaction between *A* and *B* species. The interactions between *A*-*C* and *B*-*C* pairs are assumed to be sufficiently weak. Therefore this mixture is expected to undergo phase separation between *A*-rich and *B*-rich domains at low temperatures as an ordinary spinodal decomposition. The characteristic feature of the mixture is the presence of the following hypothetical reaction among the three components:

$$A \overset{\gamma_1}{\rightarrow} B \overset{\gamma_2}{\rightarrow} C \overset{\gamma_3}{\rightarrow} A, \tag{1}$$

where γ_1, γ_2, and γ_3 are the reaction rates.

Equation (1) is a simplified representation. It should be noted that other chemical species are associated with the reactions such that, for example, $A+D \rightarrow B+E$ without violating any thermodynamic requirements. The amount of the species *D* and *E* is assumed to be controlled sufficiently fast so that these are constant in space and time.

When the incompressibility condition with a proper normalization $\psi_A+\psi_B+\psi_C=1$ is imposed, two of these variables are chosen to be independent, where ψ_X ($X=A$, *B*, and *C*) is the local volume fraction of the component *X*. Hence we define the local kinetic variables $\psi(\mathbf{r},t)$ and $\phi(\mathbf{r},t)$ at position $\mathbf{r}$ and time *t* as $\psi=\psi_A-\psi_B$ and $\phi=\psi_A+\psi_B$. The kinetic equations for these variables are given by [8]

$$\frac{\partial \psi}{\partial t} = \nabla^2 \frac{\delta F}{\delta \psi} + f(\psi,\phi), \tag{2}$$

$$\frac{\partial \phi}{\partial t} = g(\psi,\phi), \tag{3}$$

where *F* is the free-energy functional of the Ginzburg-Landau type given by

$$F = \int d\mathbf{r}\left[\frac{D}{2}|\nabla\psi|^2 - \frac{\tau}{2}\psi^2 + \frac{1}{4}\psi^4\right], \tag{4}$$

where *D* is a positive coefficient. The parameter τ is also positive in the phase-separated state. The last terms of Eqs. (2) and (3) arise from the chemical reaction (1). From the mass action law these terms are given by

$$f(\psi,\phi) = -\left(\gamma_1+\frac{\gamma_2}{2}\right)\psi - \left(\gamma_1-\frac{\gamma_2}{2}+\gamma_3\right)\phi + \gamma_3, \tag{5}$$

$$g(\psi,\phi) = \frac{\gamma_2}{2}\psi - \left(\frac{\gamma_2}{2}+\gamma_3\right)\phi + \gamma_3. \tag{6}$$

Note that the nonlinearity appears only through the free energy (4) in the present model system.

We have made several simplifications for the time-evolution equations (2) and (3) and the free energy (4). First of all, a possible coupling between ψ and ϕ through, for example, the ϕ dependence of τ in the free energy has been omitted. Second, the gradient term of ϕ is also not considered in the free energy. Finally the diffusion term has been ignored in Eq. (3). The Cahn-Hilliard-type equation with an additive term (2) is responsible for the formation of motionless periodic structures [12,13]. We have indeed verified numerically that the diffusion of ϕ does not affect qualitatively the dynamics of patterns [8]. Therefore, we believe that these simplifications would not alter the results obtained, since phase separation and the cyclic reaction are most important for the self-organized propagation of domains.

The stationary uniform solutions ψ_0 and ϕ_0 for Eqs. (2) and (3) are given, respectively, by

$$\psi_0 = \frac{\gamma_3(\gamma_2-\gamma_1)}{\gamma_1\gamma_2+\gamma_2\gamma_3+\gamma_3\gamma_1}, \tag{7}$$

$$\phi_0 = \frac{\gamma_3(\gamma_2+\gamma_1)}{\gamma_1\gamma_2+\gamma_2\gamma_3+\gamma_3\gamma_1}. \tag{8}$$

The linear stability diagram for these solutions is shown in the τ-γ_2 plane in Fig. 1 for $D=1$, $\gamma_1=0.3$, and $\gamma_3=0.05$ [8]. The solid line is an instability line where the eigenvalue for the linearized equation is complex and the real part vanishes at a certain finite wave number of the deviations. As mentioned in the Introduction, we call this a Hopf-type bifurcation throughout this paper. Another instability occurs along the dashed line such that the eigenvalue is real and it changes sign at a certain finite wave number. This bifurcation is called a Turing-type bifurcation to distinguish it from the ordinary Turing instability [14].

Now we impose the time dependence of the reaction rate γ_3 as

$$\gamma_3(t) = \overline{\gamma_3} + a\sin(\Omega t), \tag{9}$$

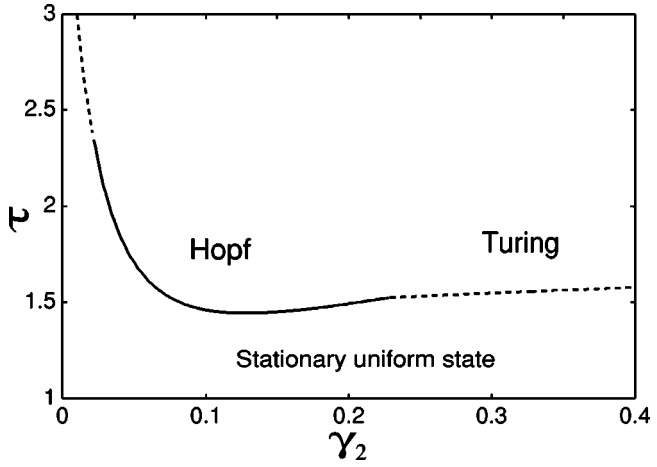

FIG. 1. Bifurcation diagram in the (γ_2, τ) plane for $D=1$, $\gamma_1=0.3$, and $\gamma_3=0.05$. The solid and dashed lines show, respectively, the lines at which the Hopf-type and Turing-type instabilities occur. The units of the horizontal and vertical axes are dimensionless in this and all the figures below.

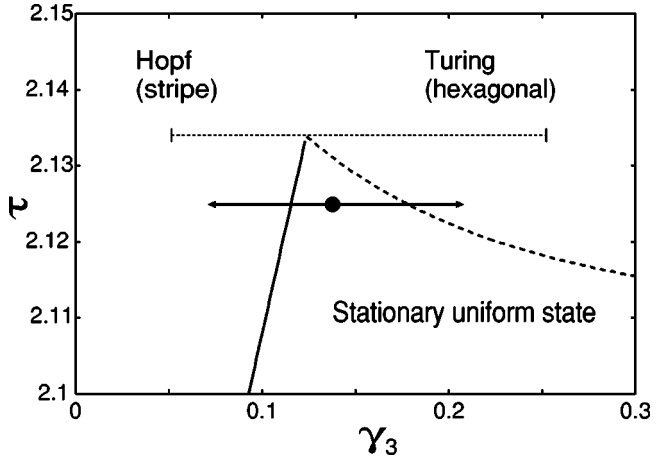

FIG. 2. Bifurcation diagram in the (γ_3, τ) plane for $D=1$, $\gamma_1=0.6$, and $\gamma_2=0.4$. The dot shows the stable uniform state at $\gamma_3=0.146\,58$ and $\tau=2.125$. The arrows indicates the temporal change of the time-dependent γ_3. The dotted line is the line for $\tau=2.134$, which is close to the multiple bifurcation point.

where a and Ω are the amplitude and the frequency of modulation, respectively. We are concerned with how the oscillation of phase-separated domains is affected by this temporal modulation. The reason why the reaction rate γ_3 is made time dependent comes from the fact that it is most convenient to traverse periodically the Hopf-type and Turing-type instability regions and the uniform state, as will be shown in the following section.

III. NUMERICAL SIMULATIONS

We have carried out computer simulations of Eqs. (2) and (3) with Eq. (9) in two dimensions. The system is discretized into 128×128 square cells. Each mesh size δx is set as $\delta x=0.5$. In most of simulations, the time increment δt is set to be $\delta t=0.001$. We have employed the Euler scheme for computation by verifying the accuracy by changing δt. The periodic boundary conditions are imposed at the system boundaries. We start with the initial conditions such that ψ and ϕ are distributed at each mesh point randomly in the interval ±0.01 around the average values ψ_0 and ϕ_0.

We have explored the domain oscillation by changing the parameters systematically and have found that the most interesting dynamics appears near the multiple bifurcation point indicated in Fig. 2, where the Turing-type bifurcation line (the dashed line) and the Hopf-type bifurcation line (the solid line) meet each other. The domain dynamics near the multiple bifurcation point have been studied numerically in a slightly different parameter space in a previous paper [8].

In order to make the present paper self-contained, we describe here some of the results without external modulations. We have carried out simulations along the dotted line in Fig. 2 for $\tau=2.134$ and for $\gamma_3=0.05$, 0.1, 0.12, 0.1236, 0.13, 0.15, 0.2, and 0.25. The asymptotic domain dynamics are as follows. When $\gamma_3=0.05$, we have propagating stripes. For $\gamma_3=0.1$ an oscillation of domains is observed. What happens in this case is a periodic appearance of the three domain patterns as shown in Fig. 3. For $\gamma_3=0.12$, a traveling hexagonal structure appears. When the value of γ_3 is increased further, we have motionless hexagons. These are obtained starting with the initial conditions mentioned above. We have also carried out simulations using a different condition. That is, we start with the asymptotic stripe pattern for $\gamma_3=0.05$ and then increase γ_3 to see the asymptotic structure repeating this up to $\gamma_3=0.25$. This procedure has also been performed by decreasing γ_3 from 0.25 to 0.05. The obtained asymptotic dynamics is essentially the same for the two methods. This indicates that any bistability of the solutions, i.e., coexistence of the different solutions, is quite unlikely near the multiple bifurcation point. We have confirmed this property even for the higher value of $\tau=2.143$.

In the simulations shown below in the presence of the external modulation, the parameters are fixed as $\gamma_1=0.6$, $\gamma_2=0.4$, and $\tau=2.125$. The constant part $\bar{\gamma}_3$ and the amplitude a in Eq. (9) are chosen such that, the system is in the uniform stable state when the external modulation is absent, and enters into the Turing-type instability region and the Hopf-type instability region periodically in time when the modulation is present as shown by the arrows in Fig. 2. It is noted that when the external modulation is turned off, a stationary hexagonal structure of domains exists in the Turing-type instability region, whereas traveling stripe domains emerge in the Hopf-type instability region.

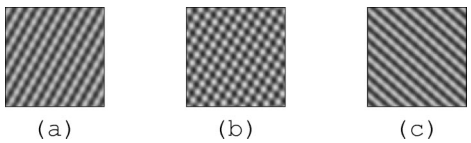

FIG. 3. Snapshots of the domain at $t=48\,690$ (a), 48 695 (b), and 48 705 (c) for $\tau=2.134$, $\gamma_1=0.6$, $\gamma_2=0.4$, and $\gamma_3=0.1$. These patterns appear periodically. In these snapshots as well as in those in the figures below, the region where ψ is large (small) is shown by white (black).

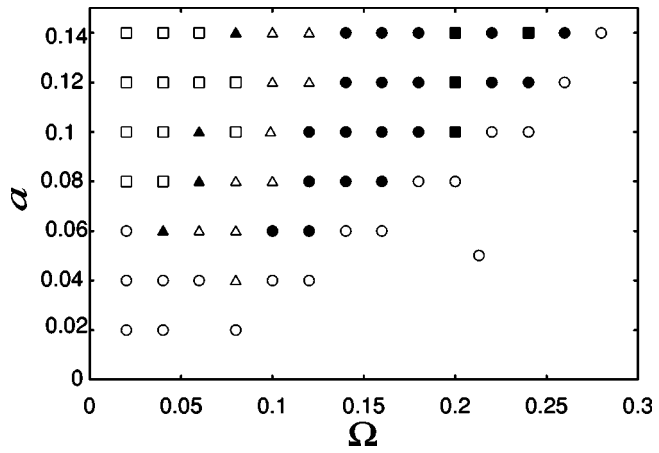

FIG. 4. Phase diagram in the space of the frequency Ω and the amplitude a of the external modulation. Other parameters are set to be $\gamma_1=0.6$, $\gamma_2=0.4$, $\overline{\gamma_3}=0.146\,58$, and $\tau=2.125$. The white circles indicate the region where the system is entrained by the external modulation but without any spatial structures. In the region of the black disks an oscillating stripe structure appears. At the parameters shown by the black squares, the stripe is not straight but bended. Oscillations of hexagons appear in the regions of both the white triangles and the black triangles. A more complicated domain oscillation appears in the region of the white squares. See the text for the ratio of the oscillating frequency of domains to the external frequency Ω.

Figure 4 is the phase diagram in the Ω-a space obtained numerically for the fixed value $\overline{\gamma_3}=0.146\,58$. In the area indicated by the white circles, the uniform oscillation with no spatial structure appears. The temporal changes of ψ and ϕ are displayed in Fig. 5 together with the external modulation $\gamma_3(t)$. It is evident that ϕ exhibits an almost in-phase oscillation with $\gamma_3(t)$, whereas the phase difference between ψ and $\gamma_3(t)$ is about $\pi/2$. Note that the critical frequency at the Hopf-type bifurcation line is given by $\omega_c=0.15$ with this set of parameters. Therefore the phase diagram implies that the external temporal modulation suppresses the traveling waves and the spatial structures when the modulation frequency is sufficiently large.

By decreasing the value of Ω for a fixed value of the amplitude a, spatially periodic structures appear and these patterns are synchronized with the external oscillation of $\gamma_3(t)$. In the region indicated by the black disks in Fig. 4, we have a standing wave of stripe domain pattern. Figure 6 displays the behavior of oscillation during two cycles of the external modulation. Here it is emphasized that the frequency ω of the domain oscillation is related with that of the external modulation as $\omega/\Omega=1/2$. That is, after one cycle the system returns to the stripe pattern but there is an antiphase relation with the initial stripes. In one more cycle of oscillation, the pattern becomes identical with the original structure.

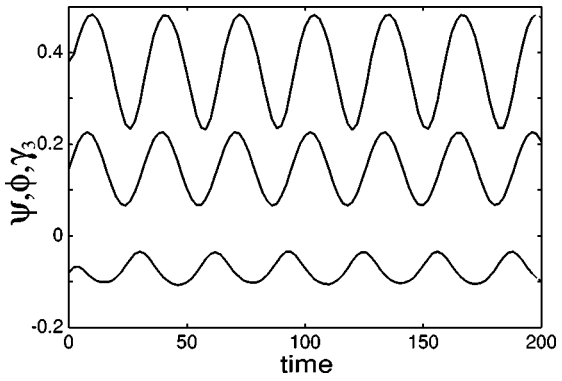

FIG. 5. The temporal changes of ψ (lower line), ϕ (upper line), and $\gamma_3(t)$ (middle line) at the center of the system when the system is uniformly entrained by the external modulation.

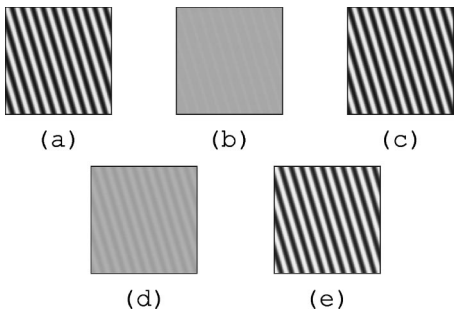

FIG. 6. Snapshots of the standing oscillation of stripes at $t=2210$ (a), 2244 (b), 2262 (c), 2296 (d), and 2310 (e) for $a=0.08$ and $\Omega=0.12$. The panels from (a) to (c) and (c) to (e) correspond to one cycle of γ_3. Note that the stripes (c) are spatially antiphase compared to those of (a) so that one cycle of domain oscillation is completed from (a) to (e).

If the external frequency is decreased further, i.e., for the parameters indicated by the white triangles in Fig. 4, the asymptotic domain pattern changes from the stripe pattern to the hexagonal one, which exhibits a standing oscillation as shown in Fig. 7. The period of oscillation in this case is also twice the external period. The reason why the morphological change occurs by changing only the frequency originates from the fact that, as mentioned above, hexagonal and lamellar structures exist above the Turing-type and Hopf-type bifurcations, respectively, in the absence of the external oscillation. However, it is noted that the dynamical behavior is quite different from the simple expectation that the hexago-

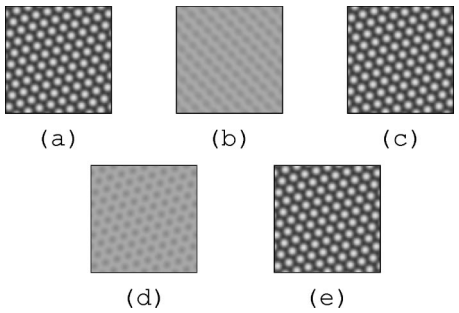

FIG. 7. Snapshots of the oscillating hexagons at $t=2220$ (a), 2262 (b), 2298 (c), 2340 (d), and 2376 (e) for $a=0.08$ and $\Omega=0.08$. The figures from (a) to (c) and (c) to (e) correspond to one cycle of γ_3. Note that the hexagons (c) are spatially antiphase compared to (a) so that one cycle of domain oscillation is completed from (a) to (e).

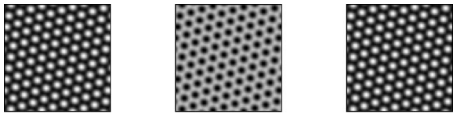

FIG. 8. Snapshots of the standing oscillation of hexagons at $t=2600$ (a), 2654 (b), and 2704 (c) for $a=0.08$ and $\Omega=0.06$ having the frequency ratio $\omega/\Omega=1$.

nal pattern appears when γ_3 is large, whereas the stripe pattern appears when γ_3 is small. In fact, Figs. 6 and 7 indicate that both stripe and hexagonal patterns appear in the interval when the reaction rate γ_3 is large. This implies that the ratio of the characteristic time of domain evolution in the absence of the external modulation to the residence time in the presence of the external modulation plays a crucial role in these domain oscillations. A mathematical formulation of this is, however, beyond the scope of the present study.

When the frequency Ω of the external modulation is smaller than about 0.055 for $a=0.08$, the oscillatory behavior changes qualitatively. At the parameters indicated by the black triangles, the oscillation of hexagons is entrained by the external modulation. In this case, however, the period of the domain oscillation turns out to be equal to that of the external modulation. From the time evolution of domain shapes shown in Fig. 8, one notes that the center of gravity of each hexagon does not move but only the amplitude of the structure oscillates coherently with the external modulation.

These two different oscillations of hexagons without propagation can be expressed by the following equations by assuming a sinusoidal spatiotemporal evolution which is found to be a good approximation in the present simulations. The case of Fig. 7 is given by

$$\psi=\psi_0+Ah(\mathbf{r})\cos(\Omega t+c), \tag{10}$$

whereas the motion shown in Fig. 8 is expressed as

$$\psi=\psi_0+Ah(\mathbf{r})\cos^2(\Omega t+c), \tag{11}$$

where ψ_0, A, and c are constants and

$$h(\mathbf{r})=\cos(\mathbf{q}_1\cdot\mathbf{r})+\cos(\mathbf{q}_2\cdot\mathbf{r})+\cos(\mathbf{q}_3\cdot\mathbf{r}), \tag{12}$$

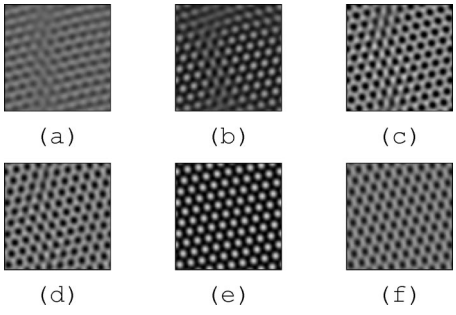

FIG. 9. Snapshots of the oscillating domains at $t=2320$ (a), 2402 (b), 2478 (c), 5780 (d), 5854 (e), and 5938 (f), for $a=0.08$ and $\Omega=0.04$. Panels (a), (b), and (c) show the evolution during one cycle of the external modulation and panels (d), (e), and (f) display the evolution of another cycle of modulation.

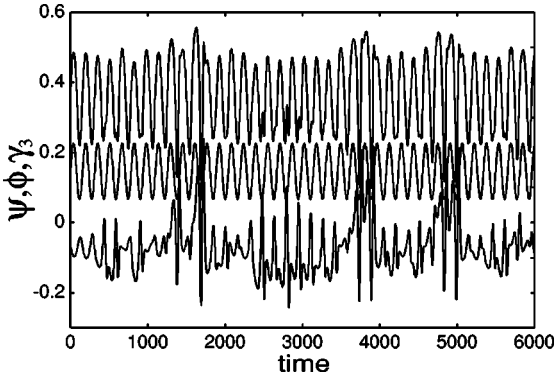

FIG. 10. The temporal changes of ψ (lower line), ϕ (upper line), and $\gamma_3(t)$ (middle line) for $a=0.08$ and $\Omega=0.04$ at the center of the system.

with $\mathbf{q}_n$ $(n=1,2,3)$ the fundamental reciprocal lattice vectors of the hexagonal pattern.

In the parameter region indicated by the white squares in Fig. 4, a complicated dynamical behavior appears. After one cycle of the external modulation, the domain pattern almost recovers the original one. For a long interval, however, several different patterns emerge and disappear without any apparent regularity. An example is displayed in Fig. 9 where pattern evolution in one period at two different times is displayed. The time evolutions of ψ and ϕ at the center of the system are plotted in Fig. 10. It seems that the system is not synchronized completely with the external modulation. In order to examine the time evolution shown in Fig. 10 in greater detail, we have plotted in Fig. 11 the values of ψ and ϕ at every T period of the external modulation. The data points are found to be accumulated on a line, indicating that the evolution is not chaotic. It is more likely that the temporal change of these quantities is quasiperiodic.

Before closing this section, we show an example of domain oscillation away from the multiple bifurcation point. Figure 12 displays the traveling hexagons modulated by the periodic external disturbance where the parameters are cho-

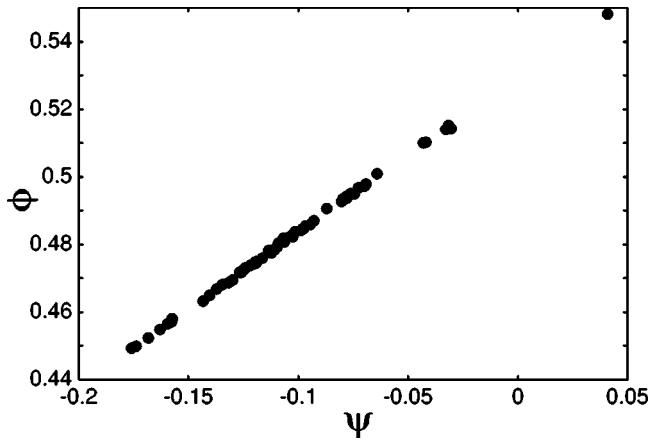

FIG. 11. Poincaré map of (ψ,ϕ) every one period of $\gamma_3(t)$ at the instant that it takes the maximum value. The data points cover from $t=628$ to 9896. Other parameters are set as $\gamma_1=0.6$, $\gamma_2=0.4$, $a=0.08$, and $\Omega=0.04$.

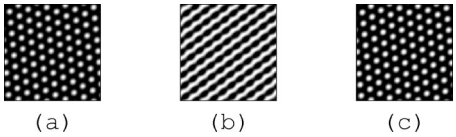

FIG. 12. Hexagons traveling to the lower right corner under the external modulation at $t=9650$ (a), 9682 (b), and 9700 (c) for $\tau=2.1$, $\gamma_1=0.6$, $\gamma_2=0.2$, $\overline{\gamma_3}=0.1$, $a=0.08$, and $\Omega=0.12$.

sen as $\tau=2.1$, $\gamma_1=0.6$, $\gamma_2=0.2$, $\overline{\gamma_3}=0.1$, $a=0.08$, and $\Omega=0.12$. As displayed in Fig. 12, the traveling hexagons are not destabilized away from the multiple bifurcation point but their amplitudes are simply modulated.

IV. THEORETICAL ANALYSIS

In order to understand the results obtained by simulations, we here make a theoretical analysis of the evolution equations (2) and (3). A uniform solution of Eqs. (2) and (3) satisfies the following set of equations,

$$\frac{\partial\psi}{\partial t}=-\left(\gamma_1+\frac{\gamma_2}{2}\right)\psi-\left[\gamma_1-\frac{\gamma_2}{2}+\gamma_3(t)\right]\phi+\gamma_3(t), \tag{13}$$

$$\frac{\partial\phi}{\partial t}=\frac{\gamma_2}{2}\psi-\left[\frac{\gamma_2}{2}+\gamma_3(t)\right]\phi+\gamma_3(t). \tag{14}$$

Equations (13) and (14) have an asymptotically periodic solution $\psi=\psi_0(t)$ and $\phi=\phi_0(t)$ as $t\to\infty$ with the period $T\equiv 2\pi/\Omega$. We have verified numerically that this solution is indeed the stable solution of Eqs. (13) and (14).

We are concerned with the stability of the uniformly oscillating solution $\psi_0(t)$ and $\phi_0(t)$ when spatially nonuniform perturbations are present. We introduce the deviations $\psi_1(\mathbf{r},t)$ and $\phi_1(\mathbf{r},t)$ around the uniform periodic solutions as

$$\psi(\mathbf{r},t)=\psi_0(t)+\psi_1(\mathbf{r},t), \tag{15}$$

$$\phi(\mathbf{r},t)=\phi_0(t)+\phi_1(\mathbf{r},t), \tag{16}$$

and write $\psi_1(\mathbf{r},t)=\alpha(t)\exp(i\mathbf{q}\cdot\mathbf{r})$ and $\phi_1(\mathbf{r},t)=\beta(t)\exp(i\mathbf{q}\cdot\mathbf{r})$. Substituting these into Eqs. (2) and (3), we obtain, up to the linear order of $\mathbf{x}\equiv(\alpha(t),\beta(t))^T$,

$$\frac{d\mathbf{x}}{dt}=L_q(t)\mathbf{x}, \tag{17}$$

where

$$L_q(t)\equiv\begin{pmatrix} -Dq^4+\tau q^2-3\psi_0^2(t)q^2-\gamma_1-\frac{\gamma_2}{2} & -\gamma_1+\frac{\gamma_2}{2}-\gamma_3(t) \\ \frac{\gamma_2}{2} & -\frac{\gamma_2}{2}-\gamma_3(t) \end{pmatrix}. \tag{18}$$

Let us introduce a fundamental solution matrix $X(t)\equiv(\mathbf{x}_1,\mathbf{x}_2)$ in terms of the independent solutions $\mathbf{x}_1$ and $\mathbf{x}_2$ of Eq. (17). $X(t)$ obeys

$$\frac{dX}{dt}=L_q(t)X. \tag{19}$$

Since $L_q(t)$ is T periodic, the solution $X(t)$ must satisfy

$$X(t+T)=MX(t). \tag{20}$$

The 2×2 matrix M is formally defined by

$$M=\mathcal{T}\exp\left[\int_t^{t+T}L_q(s)ds\right], \tag{21}$$

where $\mathcal{T}\exp[\ ]$ is the time-ordered exponential. We have solved Eqs. (13), (14), and (19) numerically by changing the wave number q to evaluate each component of the matrix M and its eigenvalues. If the real part of the eigenvalue is larger than 1 for some finite interval of q, the recurrence equation (20) means that $X(t)$ is divergent, indicating that the uniformly oscillating solution is unstable. This actually happens with the parameters shown by the black squares in Fig. 13, where the eigenvalue becomes larger than 1 in one period of the external modulation. This corresponds to the region indicated by the white squares and the black triangles in Fig. 4. The region of the white squares in Fig. 13 is a region where the eigenvalue is smaller than unity after one period, but exceeds unity after two periods. This corresponds to the region shown by the white triangles and the black disks in Fig. 4. The region with no symbols in Fig. 13 is the region where

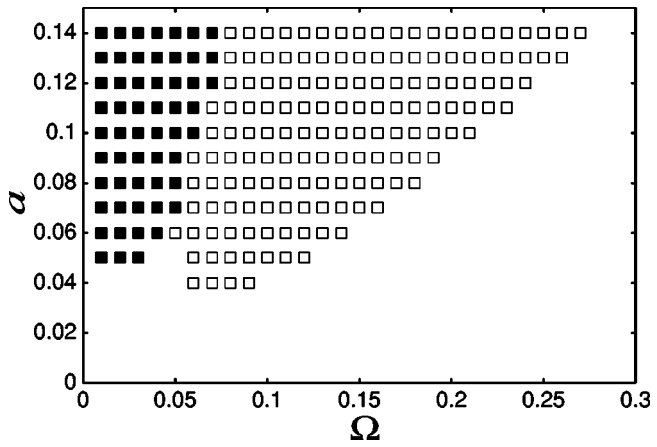

FIG. 13. Phase diagram in the Ω-a plane obtained theoretically. The black squares indicate the region where the real part of the eigenvalue is larger than 1 in one period of the external modulation, whereas the white squares indicate the region where the eigenvalue exceeds unity after two periods of the external modulation.

the real part of the eigenvalue is always smaller than 1 and hence the uniform solution is stable. Therefore, comparing Figs. 13 and 4, one notes that the theoretical results on the frequency of oscillations are in an almost complete agreement with the simulations.

V. DISCUSSION AND CONCLUDING REMARKS

We have investigated dynamics of phase-separated domains in reactive mixtures. The cyclic chemical reaction makes the system out of equilibrium and the traveling waves of domains are self-organized when no external modulation is applied. Our main concern in the present paper was to study the synchronization of self-organized patterns by applying time-modulated reaction rates. Synchronization is one of the major problems far from equilibrium. Many theoretical and experimental studies have been available for oscillatory systems such as nonlinear coupled oscillators, the complex Ginzburg-Landau-type amplitude equations [22], the Belousov-Zhabotinsky reaction under illumination [19], and the electrohydrodynamics instabilities in nematic liquid crystals [23].

However, most of the previous studies dealt with systems having no spatial structures [24] or, at most, Turing patterns [19]. In the present study, we have investigated the entrainment of dynamic mesoscopic structures under time modulation. Although our kinetic equations are based on hypothetical chemical reactions with phase separation, the model system can produce not only traveling stripes but also traveling hexagons when the external modulation is absent [8]. Therefore it is mostly convenient to study the effect of the modulation systematically for all the dynamic patterns, at least, in two dimensions. In fact, the main result in the present paper is that various dynamics due to synchronization emerge near the multiple bifurcation point where the Hopf-type bifurcation line and the Turing-type bifurcation line meet each other.

We have also investigated the effects of the external modulations in other parameter regions such that the system crosses periodically the Hopf-type bifurcation line or the Turing-type bifurcation line. However, we have found that traveling stripes and hexagons are not destabilized but, as shown in Fig. 12, those amplitudes are simply modulated in these situations.

The linear stability analysis of the uniformly oscillating solution has successfully accounted for the change of the frequency ratio obtained by numerical simulations. One of the remaining problems is the morphological change from lamellar to hexagonal patterns by decreasing the external frequency. We intend to return to this problem in the future.

ACKNOWLEDGMENTS

We would like to thank Professor A. S. Mikhailov for valuable discussion. This work was supported by a grant-in-aid for scientific research from the Ministry of Education, Science, Sports and Culture of Japan.

[1] M.C. Cross and P.C. Hohenberg, Rev. Mod. Phys. **65**, 851 (1993).
[2] R. Imbihl and G. Ertl, Chem. Rev. **95**, 697 (1995).
[3] A. von Oertzen, H.H. Rotermund, A.S. Mikhailov, and G. Ertl, J. Phys. Chem. B **104**, 3155 (2000).
[4] M. Hildebrand, A.S. Mikhailov, and G. Ertl, Phys. Rev. Lett. **81**, 2602 (1998).
[5] A.S. Mikhailov, M. Hildebrand, and G. Ertl, in *Coherent Structures in Classical Systems*, edited by M. Rubi *et al.* (Springer, New York, 2001), and references therein.
[6] Y. Tabe and H. Yokoyama, Langmuir **11**, 4609 (1995).
[7] R. Reigada, F. Sagués, and A.S. Mikhailov, Phys. Rev. Lett. **89**, 038301 (2002).
[8] T. Okuzono and T. Ohta (unpublished).
[9] T. Okuzono and T. Ohta, Phys. Rev. E **64**, 045201 (2001).
[10] J.D. Gunton, M. San Miguel, and P.S. Sahni, in *Phase Transitions and Critical Phenomena*, edited by C. Domb and J.L. Lebowitz (Academic Press, New York, 1983), Vol. 8.
[11] A.J. Bray, Adv. Phys. **43**, 357 (1994).
[12] M. Motoyama and T. Ohta, J. Phys. Soc. Jpn. **66**, 2715 (1997).
[13] S.C. Glotzer, E.A. Di Marzio, and M. Muthukumar, Phys. Rev. Lett. **74**, 2034 (1995).
[14] A.M. Turing, Philos. Trans. R. Soc. London, Ser. B **237**, 37 (1952).
[15] H. Riecke, J.D. Crawford, and E. Knobloch, Phys. Rev. Lett. **61**, 1942 (1988).
[16] R. Heinrichs, G. Ahlers, and D.S. Cannell, Phys. Rev. A **35**, 2761 (1987).
[17] P. Kolodner, D. Bensimon, and C.M. Surko, Phys. Rev. Lett. **60**, 1723 (1988).
[18] J. Fineberg, E. Moses, and V. Steinberg, Phys. Rev. Lett. **61**, 838 (1988).
[19] A.K. Horvath, M. Dolnik, A.P. Munuzuri, A.M. Zhabotinsky, and I.R. Epstein, Phys. Rev. Lett. **83**, 2950 (1999).
[20] A.L. Lin, M. Bertram, K. Martinez, H.L. Swinney, A. Ardekea, and G.F. Carey, Phys. Rev. Lett. **84**, 4240 (2000).
[21] F. Melo, P. Umbanhowar, and H.L. Swinney, Phys. Rev. Lett. **72**, 172 (1994).
[22] Y. Kuramoto, *Chemical Oscillation, Waves and Turbulence* (Springer, Berlin, 1984).
[23] T. Kawagishi, T. Mizuguchi, and M. Sano, Phys. Rev. Lett. **75**, 3768 (1995).
[24] A. Pikovsky, M. Rosenblum, and J. Kurths, *Synchronization* (Cambridge University Press, London, 2001).